

Supporting Information:

JA047438+

Design of Potent, Conformationally Constrained Smac Mimetics

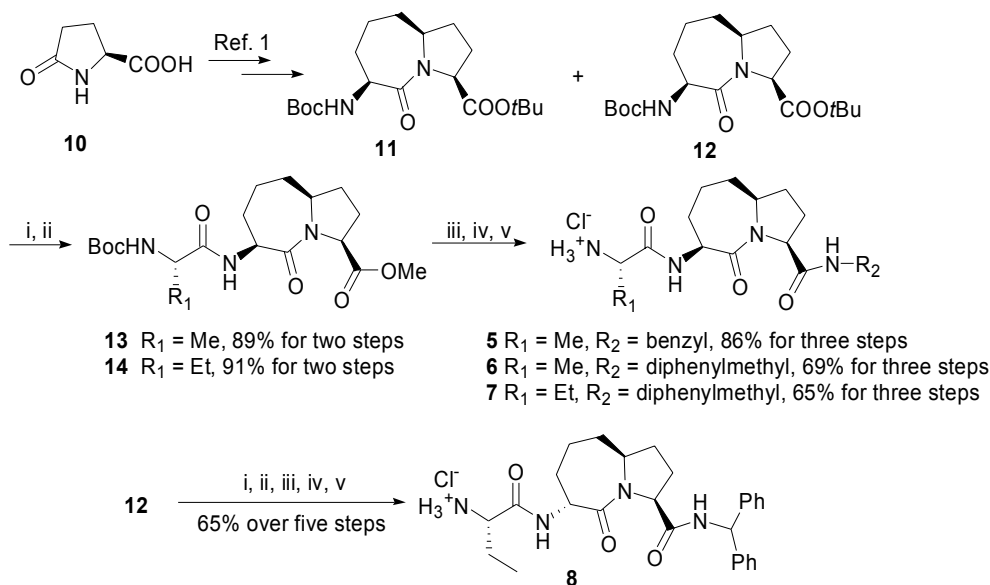
Haiying Sun,⁺ Zaneta Nikolovska-Coleska,⁺ Chao-Yie Yang,⁺ Liang Xu,⁺ Meilan Liu,⁺
York Tomita,[#] Hongguang Pan,[#] Yoshiko Yoshioka,[#] Krzysztof Krajewski,[¶] Peter P.
Roller,[¶] and Shaomeng Wang^{+*}

⁺Departments of Internal Medicine and Medicinal Chemistry and Comprehensive Cancer Center,
University of Michigan, 1500 E. Medical Center Dr., Ann Arbor, MI 48109, USA; [#]Lombardi
Cancer Center, Georgetown University Medical Center; [¶]Laboratory of Medicinal Chemistry,
National Cancer Institute-Frederick, National Institutes of Health, Frederick, Maryland 21702

I. Chemistry

The general synthesis for compounds **5**, **6**, **7** and **8** are provided in **Scheme I**. Briefly, the key intermediates **11** and **12** were prepared according to a literature reported method.¹ Treatment of **11** with saturated HCl in methanol followed by condensation with *N*-Boc-*L*-alanine or *N*-Boc-*L*-Abu gave two amides **13** and **14**. Hydrolysis of the ester groups in **13** and **14** yielded two acids. Condensation of these two acids with benzyl amine and aminodiphenyl methane, respectively, afforded three amides. Removal of the Boc protective groups in these amides furnished our desired compounds **5**, **6** and **7**. Compound **8** was synthesized according to the same sequence as that for compound **7** from intermediate **12**.

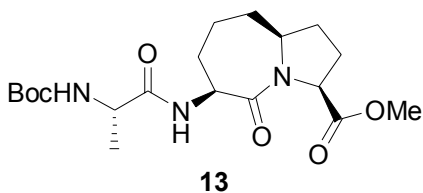
Scheme I. Synthesis of Smac mimetics **5, **6**, **7** and **8**.**



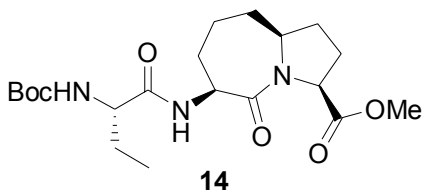
Reagents and conditions: (i) HCl (sat.) in MeOH; (ii) *N*-(*tert*-Butoxycarbonyl)-*L*-alanine or *N*-(*tert*-Butoxycarbonyl)-*L*-2-amino-butylric acid, EDC, HOBT, *N,N*-diisopropylethylamine, CH₂Cl₂, rt; (iii) 2 N LiOH, 1,4-dioxane, 0°C - rt, then 1 N HCl; (iv) benzyl amine or aminodiphenylmethane, EDC, HOBT, *N,N*-diisopropylethylamine, CH₂Cl₂, rt; (v) 4 N HCl in 1, 4-dioxane, MeOH.

General Methods: NMR spectra were acquired at a proton frequency of 300 MHz. ¹H chemical shifts are reported with DHO (4.70 ppm) as internal standards. ¹³C chemical

shifts are reported with 1, 4-dioxane (67.16 ppm) as internal standards. The final products were purified by a C18 reverse phase semi-preparative HPLC column with solvent A (0.1% of TFA in water) and solvent B (0.1% of TFA in CH₃CN) as eluents.

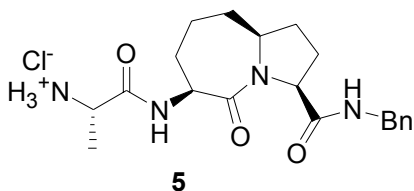


Compound **11** (370 mg, 1 mmol) was dissolved in 5 mL of a solution of saturated HCl in MeOH. The resulting solution was stirred at room temperature overnight and then condensed in vacuo to give the crude ammonium salt. To a mixture of this salt (160 mg, 0.61 mmol) in 10 mL of CH₂Cl₂ was added *N*-(*tert*-butoxycarbonyl)-L-alanine (120 mg, 0.62 mmol), EDC (140 mg, 0.72 mmol), HOBt (95 mg, 0.7 mmol) and diisopropylethyl amine (0.4 mL, 2.3 mmol) respectively at room temperature. The mixture was stirred at room temperature overnight and then condensed. The residue was purified by chromatography to give compound **13** (215 mg, 89% for two steps). ¹H NMR (300 MHz, CDCl₃) δ 7.25 (brs, 1H), 5.08 (brs, 1H), 4.65 (m, 1H), 4.46 (m, 1H), 4.08 (m, 1H), 3.87 (m, 1H), 3.77 (s, 3H), 2.27 (m, 1H), 2.08-1.52 (m, 9H), 1.46 (brs, 9H), 1.36 (d, *J* = 7.6 Hz, 3H); ¹³C NMR (75 MHz, CDCl₃) δ 172.46, 172.04, 171.59, 155.09, 79.84, 60.32, 59.17, 53.32, 52.36, 50.22, 34.17, 32.86, 31.07, 28.29, 27.60, 27.51, 19.16.

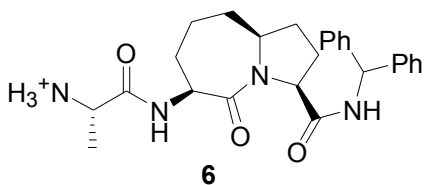


To a mixture of the crude ammonium (80 mg, 0.30 mmol) resulting from compound **11** as mentioned above in 5 mL of dry CH₂Cl₂ was added *N*-(*tert*-butoxycarbonyl)-2-aminobutyric acid (65 mg, 0.30 mmol), EDC (70 mg, 0.36 mmol), HOBt (50 mg, 0.36 mmol) and diisopropylethyl amine (0.2 mL, 1.2 mmol), respectively, at room temperature. The mixture was stirred at room temperature overnight and then condensed. The residue was purified by chromatography to give compound **14** (114 mg, 91% for two steps). ¹H NMR (300 MHz, CDCl₃) δ 7.25 (brs, 1H), 5.08 (brs, 1H), 4.65 (m, 1H), 4.46 (m, 1H), 4.08 (m,

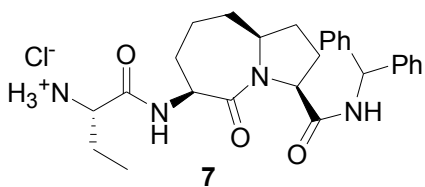
1H), 3.87 (m, 1H), 3.77 (s, 3H), 2.27 (m, 1H), 2.08-1.52 (m, 11H), 1.45 (brs, 9H), 0.93 (t, $J = 7.5$ Hz, 3H); ^{13}C NMR (75 MHz, CDCl_3) δ 172.44, 170.95, 170.85, 155.37, 79.74, 60.33, 59.18, 55.67, 53.29, 52.35, 34.16, 32.87, 31.14, 28.29, 27.59, 27.51, 26.37, 9.73.



To a well-stirred solution of compound **12** (190 mg, 0.48 mmol) in 2 mL of 1,4-dioxane was added 1 mL of an aqueous solution of 2 N LiOH at 0 °C. The mixture was stirred at room temperature until all the starting material has been consumed, then 1 N HCl was used to adjust pH to 5. Dichloromethane was used to extract the product, and the combined organic layers were washed with brine and dried over Na_2SO_4 . Removal of the solvent in vacuo gave a crude acid. The acid was used directly in the following step without further purification. To a solution of this crude acid (38 mg, 0.1 mmol) in 3 mL of CH_2Cl_2 was added benzyl amine (13 mg, 0.12 mmol), EDC (25 mg, 0.13 mmol), HOBt (18 mg, 0.13 mmol) and diisopropylethyl amine (40 mg, 0.31 mmol), respectively, at 0 °C. The mixture was stirred at room temperature overnight and then condensed. The residue was purified by chromatography to give an amide. To a solution of this amide in 3 mL of methanol was added 0.5 mL of a solution of 4 N HCl in 1,4-dioxane. The solution was stirred at room temperature overnight and then condensed to give the crude product. The crude product was purified by chromatography on a C18 reverse phase semi-preparative HPLC column and then lyophilized to give compound **6** (35 mg, 86%). Gradient ran from 90% of solvent A and 10% of solvent B to 75% of solvent A and 25% of solvent B in 40 min. The purity was confirmed by analytical HPLC to be over 98%. ^1H NMR (300 MHz, D_2O) δ 7.32-7.13 (m, 5H), 4.43 (m, 1H), 4.40 (m, 1H), 4.30 (brs, 2H), 3.98 (m, 1H), 3.93 (m, 1H), 2.18-1.51 (m, 10H), 1.44 (d, $J = 7.1$ Hz, 3H); ^{13}C NMR (75 MHz, D_2O) δ 174.52, 173.00, 170.43, 138.61, 129.39, 128.03, 127.71, 62.96, 60.26, 54.31, 49.58, 43.55, 33.46, 33.09, 29.70, 28.47, 27.61, 17.16; Anal. $\text{C}_{20}\text{H}_{29}\text{ClN}_4\text{O}_3 \cdot 0.9\text{CF}_3\text{COOH}$ required: C 51.26, H 5.90, N 10.97; found: C 51.67, H 5.93, N 10.65.



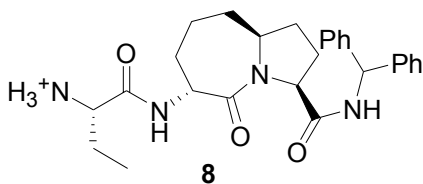
To a solution of the crude acid (42 mg, 0.11 mmol) resulting from hydrolysis of compound **12** as mentioned above in 3 mL of CH₂Cl₂ was added aminodiphenylmethane (21 mg, 0.11 mmol), EDC (25 mg, 0.13 mmol), HOBt (18 mg, 0.13 mmol) and diisopropylethyl amine (42 mg, 0.32 mmol), respectively, at 0 °C. The mixture was stirred at room temperature overnight and then condensed. The residue was purified by chromatography to give an amide. To a solution of this amide in 3 mL of methanol was added 0.5 mL of a solution of 4 N HCl in 1,4-dioxane. The solution was stirred at room temperature overnight and then condensed to give the crude product. The crude product was purified by chromatography on a C18 reverse phase semi-preparative HPLC column and then lyophilized to give compound **7** (37 mg, 69%). Gradient ran from 80% of solvent A and 20% of solvent B to 65% of solvent A and 35% of solvent B in 40 min. The purity was confirmed by analytical HPLC to be over 98%. ¹H NMR (300 M Hz, D₂O) δ 7.32-7.21 (m, 10H), 5.95 (s, 1H), 4.50-4.12 (m, 2H), 3.98 (m, 1H), 3.90 (m, 1H), 2.15-1.52 (m, 10H), 1.44 (d, *J* = 7.2 Hz, 3H); ¹³C NMR (75 MHz, D₂O) δ 173.79, 172.91, 170.42, 141.58, 141.40, 129.59, 129.49, 128.44, 128.40, 127.95, 127.78, 62.75, 60.20, 58.29, 54.30, 49.61, 33.44, 33.12, 29.72, 28.45, 27.60, 17.17; Anal. C₂₆H₃₃ClN₄O₃·0.9CF₃COOH required: C 56.90, H 5.82, N 9.55; found: C 57.20, H 5.85, N 9.38.



To a mixture of compound **13** (62 mg, 0.15 mmol) in 2 mL of 1,4-dioxane was added 0.5 mL of an aqueous solution of 2 N LiOH at 0 °C. The mixture was stirred at room temperature until all the starting material had been consumed, then 1 N HCl was used to adjust pH to 5. Dichloromethane was used to extract the product, and the combined

organic layers were washed with brine and dried over Na₂SO₄. The solution was evacuated in vacuo to give a crude acid. To a solution of this crude acid in 3 mL of CH₂Cl₂ was added aminodiphenylmethane (30 mg, 0.16 mmol), EDC (35 mg, 0.18 mmol), HOBt (25 mg, 0.18 mmol) and diisopropylethyl amine (50 mg, 0.38 mmol), respectively, at 0 °C.

The mixture was stirred at room temperature overnight and then condensed. The residue was purified by chromatography to give an amide. To a solution of this amide in 3 mL of methanol was added 0.5 mL of a solution of 4 N HCl in 1,4-dioxane. The solution was stirred at room temperature overnight and then condensed to give the crude product. The crude product was purified by chromatography on a C18 reverse phase semi-preparative HPLC column and then lyophilized to give compound **8** (48 mg, 65%). Gradient ran from 80% of solvent A and 20% of solvent B to 65% of solvent A and 35% of solvent B in 40 min. The purity was confirmed by analytical HPLC to be over 98%. ¹H NMR (300 M Hz, D₂O) δ 7.38-7.20 (m, 10H), 5.95 (s, 1H), 4.50-4.44 (m, 2H), 3.92 (m, 1H), 3.88 (m, 1H), 2.25-1.50 (m, 12H), 0.92 (t, *J* = 7.5 Hz, 3H); ¹³C NMR (75 MHz, D₂O) δ 173.75, 172.79, 169.47, 141.55, 141.38, 129.56, 129.45, 128.41, 128.37, 127.92, 127.75, 62.67, 60.19, 58.27, 54.85, 54.33, 33.40, 33.08, 29.92, 28.41, 27.59, 25.00, 9.01; Anal. C₂₇H₃₅ClN₄O₃·1.1CF₃COOH required: C 56.24, H 5.85, N 8.98; found: C 56.22, H 5.97, N 8.87.



Compound **8** can be prepared in the same sequence as that for compound **7** from compound **12**. The total for the five steps is 65%. The gradient condition for the purification of **8** is from 80% of solvent A and 20% of solvent B to 65% of solvent A and 35% of solvent B in 40 min. The purity of **8** was confirmed by analytical HPLC to be over 98%. ¹H NMR (300 M Hz, D₂O) δ 7.18-6.90 (m, 10H), 5.86 (s, 1H), 4.38 (m, 1H), 4.30 (m, 1H), 3.88 (t, *J* = 6.4 Hz, 1H), 3.77 (m, 1H), 1.95-1.42 (m, 12H), 0.85 (t, *J* = 7.5

Hz, 3H); ^{13}C NMR (75 MHz, D_2O) δ 173.11, 172.40, 170.26, 141.76, 141.70, 129.35, 129.31, 128.14, 127.81, 127.75, 63.39, 59.11, 57.88, 56.38, 54.69, 33.21, 27.95, 26.90, 25.14, 22.14, 9.04; Anal. $\text{C}_{27}\text{H}_{35}\text{ClN}_4\text{O}_3 \cdot 0.8\text{CF}_3\text{COOH}$ required: C 58.28, H 6.12, N 9.50; found: C 58.35, H 6.21, N 9.09.

II. Fluorescence Polarization Competitive Binding Assay

A sensitive and quantitative *in vitro* binding assay using the fluorescence polarization (FP) based method was developed and used to determine the binding affinity of Smac mimetics to XIAP protein.²

For this assay, 5-carboxyfluorescein (5-Fam) was coupled to the lysine sidechain of a mutated Smac peptide, AbuRPF-K-(5-Fam)- NH_2 (termed **SM5F**). The K_d value of the binding of **SM5F** peptide to XIAP BIR3 protein was determined to be 0.018 μM (17.9 nM), indicating that this peptide binds to the XIAP BIR3 protein with high affinity. The recombinant XIAP BIR3 protein of human XIAP (residues 241-356) fused to His-tag was stable and soluble, and was used for the FP based binding assay.

The dose-dependent binding experiments were carried out with serial dilutions of the tested compounds in DMSO. A 5 μl sample of a tested compound and preincubated XIAP BIR3 protein (0.030 μM) and **SM5F** peptide (0.005 μM) in the assay buffer (100 mM potassium phosphate, pH 7.5; 100 $\mu\text{g}/\text{ml}$ bovine gamma globulin; 0.02% sodium azide, purchased from InvitrogenTM Life Technology), were added in Dynex 96-well, black, round-bottom plates (Fisher Scientific) to produce a final volume of 125 μl .

For each assay, the bound peptide control containing XIAP BIR3 protein and **SM5F** (equivalent to 0% inhibition) and free peptide control containing only free **SM5F** (equivalent to 100% inhibition) were included. The polarization values were measured after 3 hrs of incubation, using an ULTRA READER (Tecan U.S. Inc., Research Triangle Park, NC). IC_{50} values, the inhibitor concentration at which 50% of bound peptide is displaced, were determined from a plot using nonlinear least-squares analysis. Curve fitting was performed using GRAPHPAD PRISM software (GraphPad Software, Inc., San Diego, CA).

To calculate the binding affinity constants (K_i) of inhibitors, we have used the following equation developed for computing the K_i values in FP-based binding assays:

$$K_i = [I]_{50} / ([L]_{50} / K_d + [P]_0 / K_d + 1)$$

in which $[I]_{50}$ denotes the concentration of the free inhibitor at 50% inhibition, $[L]_{50}$ the concentration of the free labeled ligand at 50% inhibition, $[P]_0$ the concentration of the free protein at 0% inhibition, and K_d the dissociation constant of the protein-ligand complex. For accurately computing the K_i values of inhibitors using the presented equation, we developed a computational procedure to compute the accurate values of all of the parameters required in the equation.² A Web-based computer program was also developed for computing the K_i values for inhibitors in FP-based binding assays based upon the same equation.²

III. Molecular modeling

The X-ray structure⁷ of Smac protein in complex with XIAP BIR3 was used as the initial structure for our structure-based design and molecular modeling and the structural coordinates were obtained from the Protein Data Bank (<http://www.rcsb.org/pdb/>, PDB code:1G73). The structure of the Smac AVPI peptide in complex with XIAP BIR3 domain was obtained by modifying the X-ray structure of the Smac protein in complex with XIAP BIR3 using the Sybyl program.⁸

The initial structures of designed compounds (**2**, **3**, **4**, **5**, **6**, **7**, and **8**) in complex with XIAP BIR3 were obtained by directly modifying the AVPI peptide using the Sybyl program.⁸ The initial complex structures for these designed compounds were then refined by extensive MD simulations.

The Amber program suite⁴ (version 7) was employed to perform molecular dynamics (MD) simulations to refine the complex structures between the designed compounds and XIAP BIR3 protein. The Amber force field (ff96)⁴ was used for all the natural amino acids in the complex. The TIP3P model⁵ was used for water molecules. In the XIAP BIR3 domain, a Zinc ion is covalently bonded with four residues (C300, C303, H320, and C327). This Zinc atom is important for the structural integrity of the protein but does not appear to have any direct interaction with Smac. We used parameters

developed by Ryde⁶ for the Zinc ion and its coordination with the neighboring four residues to model this chelating structure in our MD simulation. For the designed Smac mimetics, the Antechamber module implemented in the Amber program was used to derive all the necessary parameters for MD simulations.

To prepare for the MD simulation, counter ions were added to neutralize the ligand-protein complex before solvating the system with a cubic box of TIP3P water molecules. The size of the water box was 10 Å in each dimension. The four residues bonded with the Zn ion were constrained by moderate harmonic forces to prevent unfolding of the protein. The protocol of the MD simulation is as follows: A 500-step minimization of the solvated system was performed, followed by a 6 ps of MD simulation to gradually heat the system from 0 K to 298K. The system was then equilibrated by another 34 ps simulation at 298 K. Finally, the 1 ns production simulation was run and the snapshots of conformations (typically 2000) evenly spaced in time were collected for structural analysis. All the MD simulations were NTP simulation (T=298K and P = 1 atm). The SHAKE algorithm⁹ was used to fix the bonds involving hydrogen atoms. The PME method¹⁰ was used to account for long range electrostatic interaction and the non-bonded cutoff distance was set at 10 Å. The time step was 2 fs, and the neighboring pairs list was updated in every 20 steps. The structures of compounds **3**, **4**, **5** and **7** in complex with XIAP BIR3 domain obtained after 1 ns MD simulations are shown in **Figures S1, S2, S3** and **S4**.

Figure S1. Modeled structure of compound **3** (yellow) in complex with XIAP BIR3. The X-ray crystal structure of Smac AVPI peptide (green) in complex with XIAP BIR3 is superimposed on the modeled structure for comparison. Carbon atoms are shown in yellow and green for **3** and Smac AVPI, respectively; Oxygen and nitrogen atoms are shown in red and blue, respectively. Hydrogen bonds are shown in light-blue dashed lines. Note that the conformation constrained by the bicyclic ring system leads to a weaker van der Waals interaction between the proline ring and W323 while increasing potential van der Waals contacts between the six-member ring and W323.

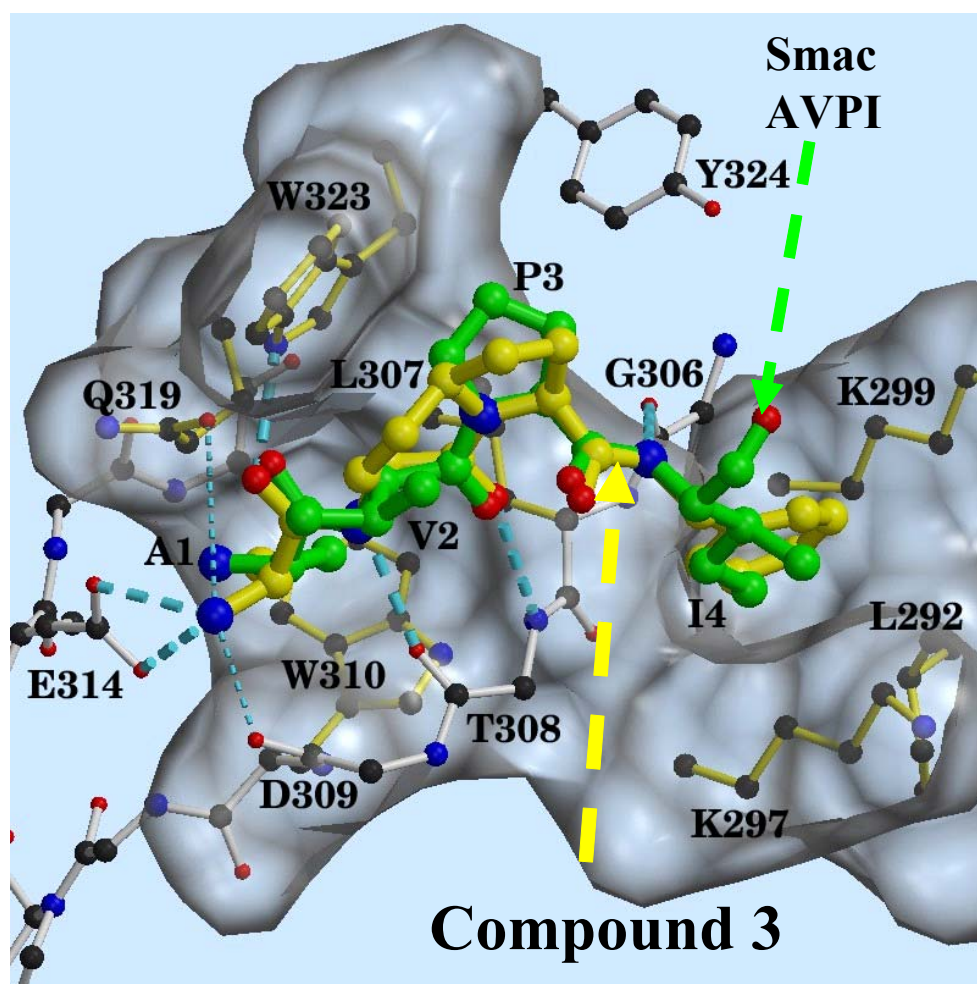


Figure S2. Modeled structure of compound **4** (yellow) in complex with XIAP BIR3. The X-ray crystal structure of Smac AVPI peptide (green) in complex with XIAP BIR3 is superimposed on the modeled structure for comparison. Carbon atoms are shown in yellow and green for **4** and Smac AVPI, respectively; Oxygen and nitrogen atoms are shown in red and blue, respectively. Hydrogen bonds are shown in light-blue dashed lines. Note that the different conformation constrained by the bridging carbon atom leads to the disruption of hydrogen bond between compound **4** and G306 and exposing the phenyl ring to the solvents instead of interacting with the hydrophobic pocket formed by L292, K297 and K299.

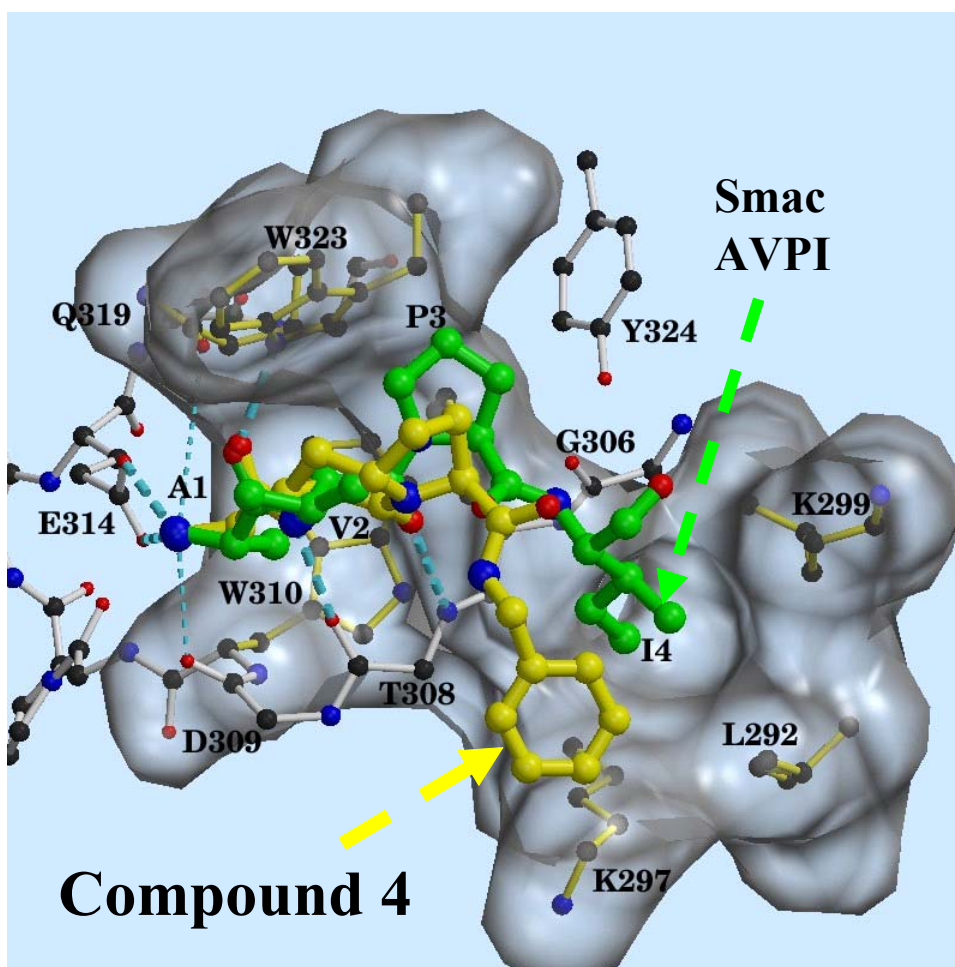


Figure S3. Modeled structure of compound **5** (yellow) in complex with XIAP BIR3. The X-ray crystal structure of Smac AVPI peptide (green) in complex with XIAP BIR3 is superimposed on the modeled structure for comparison. Carbon atoms are shown in yellow and green for **5** and Smac AVPI, respectively; Oxygen and nitrogen atoms are shown in red and blue, respectively. Hydrogen bonds are shown in light-blue dashed lines. Note that the conformation constrained by the [7,5] bicyclic ring system structurally mimics closely the AVPI peptide and increases the van der Waals contacts between the seven-membered ring and W323.

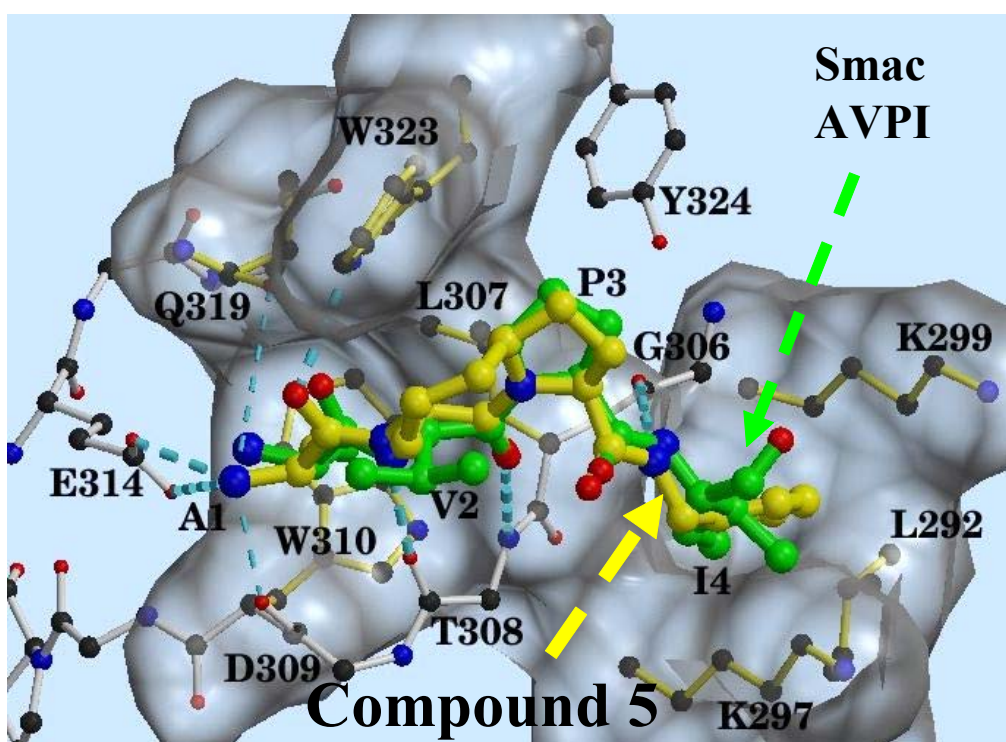
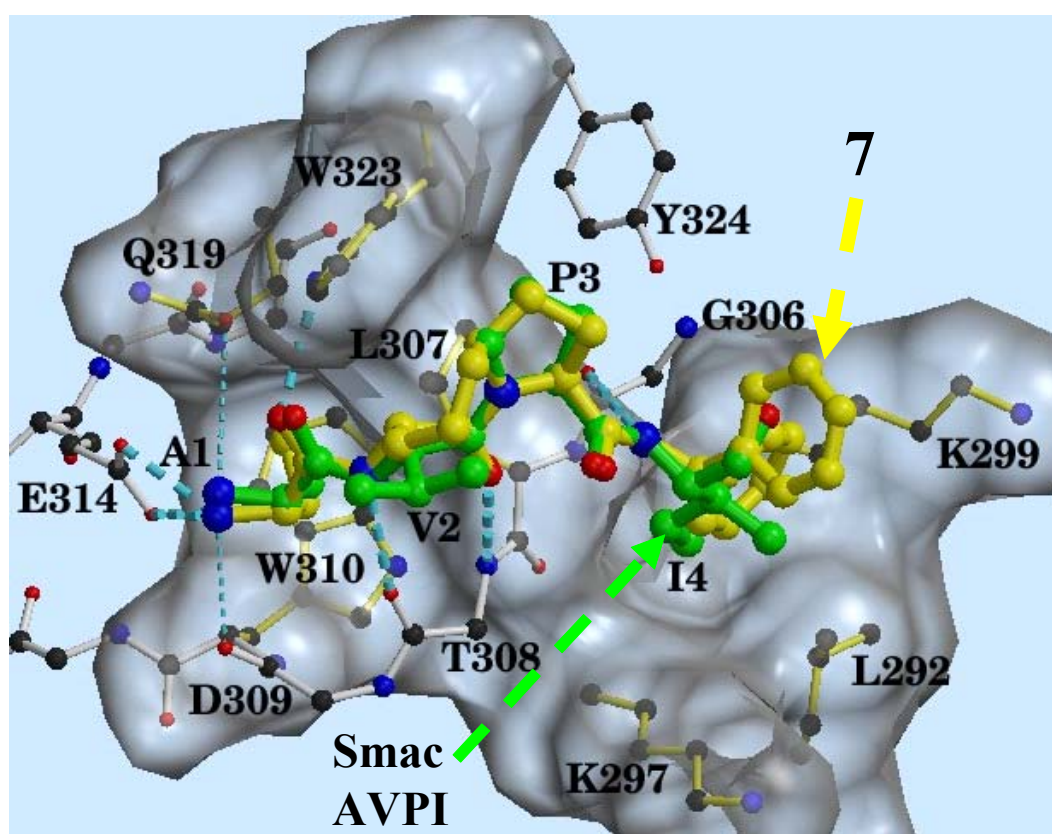


Figure S4. Modeled structure of compound **7** (yellow) in complex with XIAP BIR3. The X-ray crystal structure of Smac AVPI peptide (green) in complex with XIAP BIR3 is superimposed on the modeled structure for comparison. Carbon atoms are shown in yellow and green for **7** and Smac AVPI, respectively; Oxygen and nitrogen atoms are shown in red and blue, respectively. Hydrogen bonds are shown in light-blue dashed lines. Note that the conformation constrained by the [7,5] bicyclic ring system structurally mimics closely the AVPI peptide and increases the van der Waals contacts between the seven-membered ring and W323.



IV. NMR Heteronuclear Single Quantum Coherence (HSQC) experiments

The BIR3 domain (residues 241-356) of human XIAP fused to His-tag (pET28b, Novagen) was expressed from *E. coli* BL21(DE3) cells (Novagen) in M9 medium containing ^{15}N ammonium chloride to uniformly label protein with ^{15}N , or ^{13}C Glucose and ^{15}N ammonium chloride to uniformly double label protein with ^{13}C and ^{15}N . Most of the protein was found in the soluble fraction and it was purified using TALON (Clontech) Co affinity chromatography, followed by Q-XL ionexchange and G75 size-exclusion chromatography (APB). ^{15}N HSQC NMR spectra were recorded on a Bruker DMX 500MHz NMR spectrometer with samples containing 100 μM of the ^{15}N labeled protein (for screening) or 700 μM of the $^{13}\text{C}/^{15}\text{N}$ labeled protein (for chemical shifts assignments) in 50 mM Tris (pH 7.2), 50 μM $\text{Zn}(\text{Cl})_2$, 1 mM DTT at 30 °C. The backbone atom resonance assignments were made using ^{13}C and ^{15}N double labeled XIAP-BIR3, 3D NMR triple resonance experiments (HNCA, HNCACB, HN(CO)CBCA, TOCSY-HSQC, C(CO)NH), and the published results.^{11,12} The backbone assignments are nearly complete, except for the two flexible loops (residues 276-280 and 308-314).¹¹

To conclusively confirm that **7** binds to the pocket on the XIAP BIR3 domain where Smac binds, we recorded ^{15}N HSQC NMR spectra with 70 μM of the BIR3 domain of human XIAP protein and different concentrations of Smac peptide **1** and compound **7** (0, 10, 30, 50 and 100 μM). The overlaid HSQC spectra for Smac peptide **1** and compound **7** are shown in **Figures S5** and **S6**, respectively. The HSQC spectra showed that both Smac peptide **1** and compound **7** don't unfold the protein. Based upon the backbone assignments of XIAP BIR3, it was found that the residues affected by **7** are mostly identical to the ones affected by the Smac AVPI peptide **1**, suggesting that

compounds **7** and the Smac AVPI peptide bind to XIAP BIR3 in a similar or identical manner. Both **7** and Smac peptide **1** affect crucial residues with which Smac protein interacts (L284, L292, K297, K299, G306, L307, T308, W310, Q314, Q319, and W323 in the XIAP BIR3 domain) in the experimental structures of XIAP BIR3 in complex with Smac protein or peptide.

Figure S5. Overlay of five ^{15}N HSQC spectra of the XIAP BIR3 domain (70 μM) with various concentrations of Smac AVPI peptide **1** (0, 10, 30, 50 and 100 μM). The bottom panel shows a representative of the shift of peak population with different concentrations of **1**. The peak (the white box in the full spectra) corresponds to the residue Glycine 306 in XIAP BIR3, which is in direct contact with Smac protein in the X-ray structure of Smac in complex with XIAP BIR3.⁷ Other residues influenced by Smac AVPI peptide **1** show similar behavior (i.e. slow exchange and the affected residues appear in yellow since green and blue layers are shifted away).

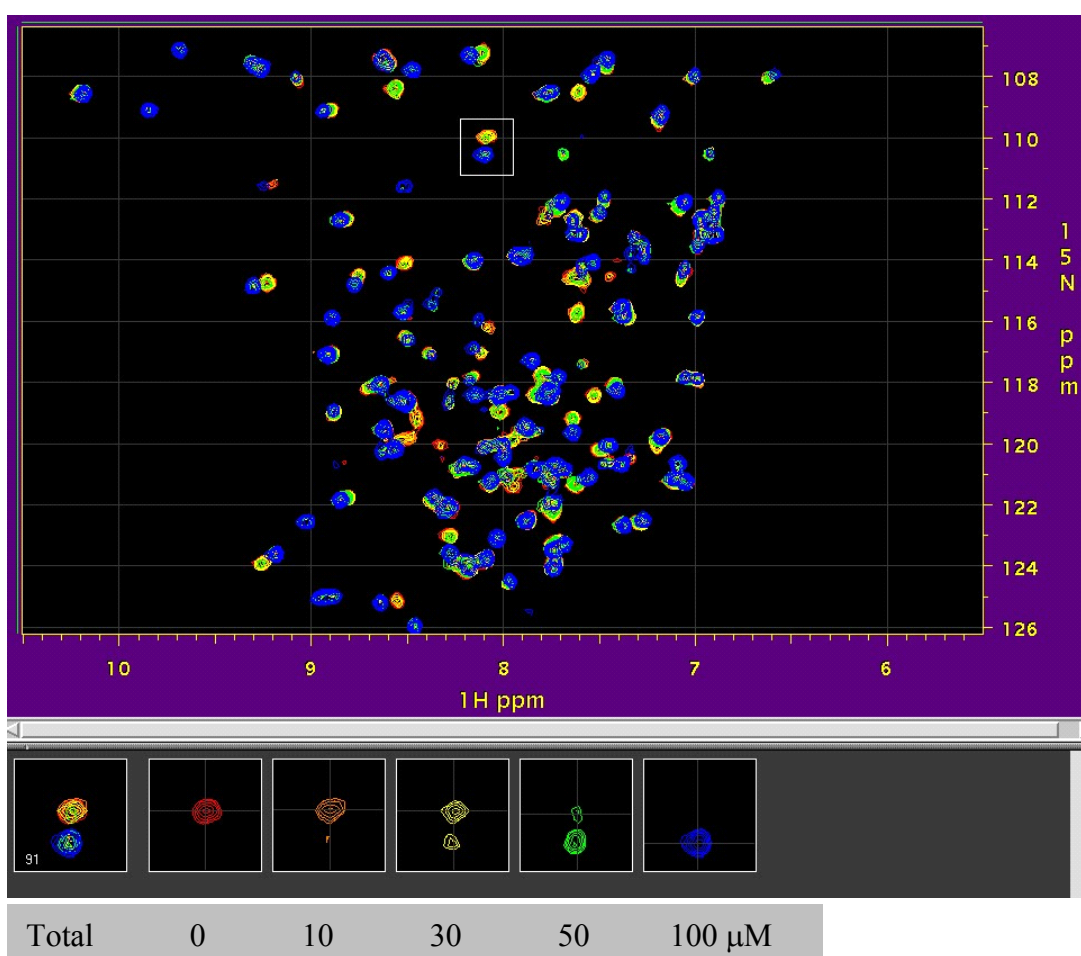
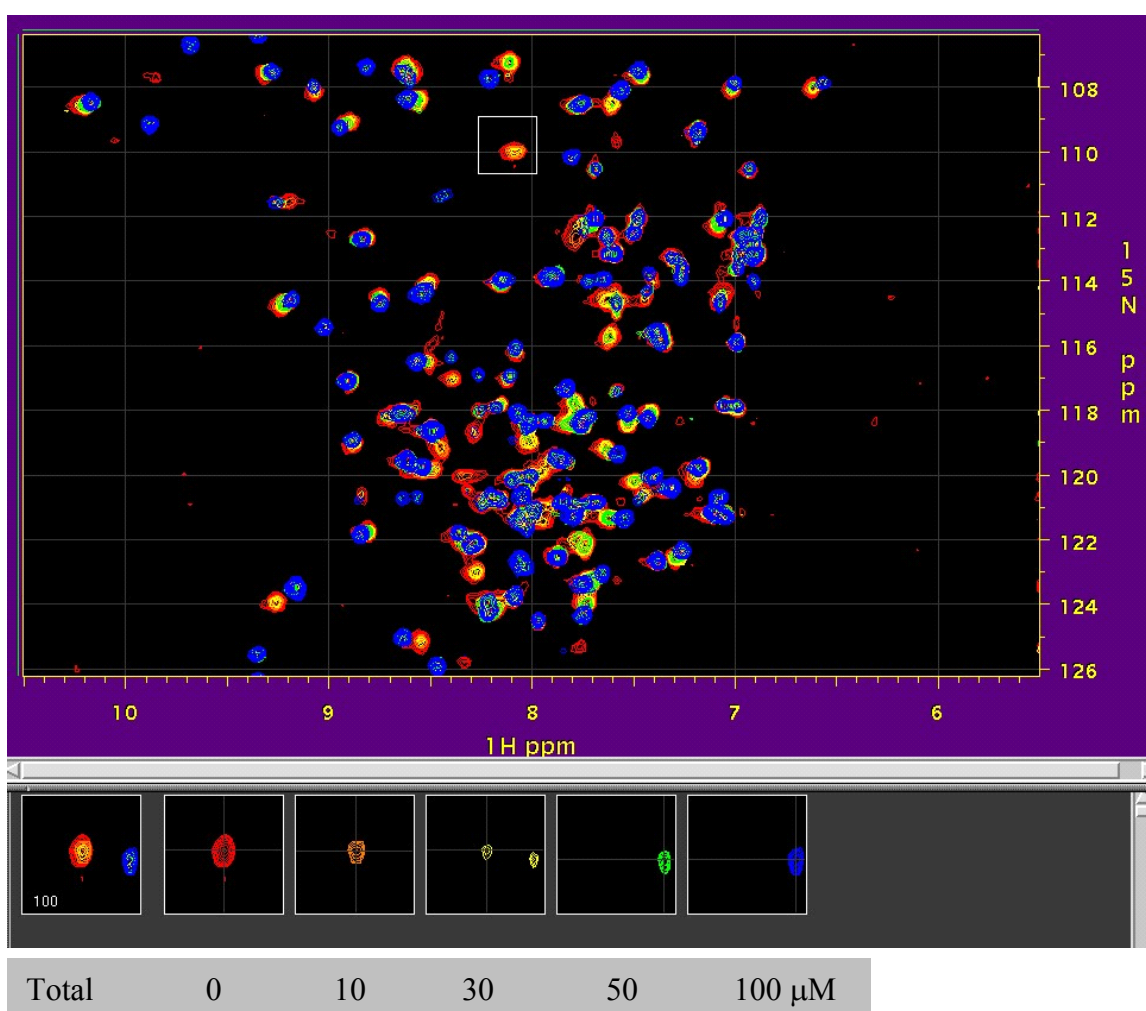


Figure S6. Overlay of five ^{15}N HSQC spectra of the XIAP BIR3 domain ($70\ \mu\text{M}$) with various concentrations of compound **7** (0, 10, 30, 50 and $100\ \mu\text{M}$). The bottom panel shows a representative of the shift of peak population with different concentrations of **7**. The peak (the white box in the full spectra) corresponds to the residue Glycine 306 in XIAP BIR3, which is in direct contact with Smac protein in the X-ray structure of Smac in complex with XIAP BIR3.⁷ Other residues influenced by Smac AVPI peptide **7** show similar behavior (i.e. slow exchange and the affected residues appear in yellow since green and blue layers are shifted away).



V. Cell growth assay

Briefly, JK-XIAP and JK-Vec cells were treated with various doses of etoposide, alone or in combination with compounds 4, 7 and a cell-permeable Smac peptide in 96-well plates in triplicates (40,000 cells/well) for 3-4 days, then 20 μ l/well WST-1 reagent was added and incubated for 2 hr. The OD450nm vs. OD650nm were measured using a plate reader and the cell growth was calculated as a % of untreated control. The detailed experimental procedure was described previously.¹³

References:

1. Angiolini, M.; Araneo, S.; Belvisi, L.; Cesarotti, E.; Checchia, A.; Crippa, L.; Manzoni, L. and Scolastico, C. Synthesis of Azabicycloalkane Amino Acid Scaffolds as Reverse-Turn Inducer Dipeptide Mimics. *Eur. J. Org. Chem.* **2000**, 2571-2581.
2. Nikolovska-Coleska, Z.; Wang, R.; Fang, X.; Pan, H.; Tomita, Y.; Li, P.; Roller, P.P.; Krajewski, K.; Saito, N.G.; Stuckey, J.A.; Wang, S. Development and optimization of a binding assay for the XIAP BIR3 domain using fluorescence polarization. *Anal Biochem.* **2004**, 332:261-73.
3. Case, D. A.; Pearlman, D. A.; Caldwell, J. W.; Cheatham III, T. E.; Wang, J.; Ross, W. S.; Simmerling, C. L.; Darden, T. A.; Merz, K. M.; Stanton, R. V.; Cheng, A. L.; Vincent, J. J.; Crowley, M.; Tsui, V.; Gohlke, H.; Radmer, R. J.; Y. Duan; Pitera, J.; Massova, I.; Seibel, G. L.; Singh, U. C.; Weiner, P. K.; Kollman, P. A. *AMBER7*, University of California, San Francisco, **2002**.
4. Kollman, P. A.; Dixon, R.; Cornell, W.; Fox, T.; Chipot, C.; Pohorille, A. In *Computer Simulation of Biomolecular Systems*, Vol. 3, Wilkinson, A.; Weiner, P. and van Gunsteren, W. F., Ed., Elsevier, **1997**, p. 83.
5. Jorgensen, W. L.; Chandrasekhar, J.; Madura, J. D.; Impey, R. W.; Klein, M. L. *J. Chem. Phys.* **1983**, 79, 926.
6. Ryde, U. *Proteins: Struct. Funct. Genet.* **1995**, 21, 41.
7. Wu, G.; Chai, J.; Suber, T. L.; Wu, J. W.; Du, C.; Wang, X.; Shi, Y. *Nature* **2000**, 408, 1008.
8. Sybyl, a molecular modeling system, is supplied by Tripos, Inc., St. Louis, MO 63144.
9. Rychaert, J. P.; Ciccotti, G.; Berendsen, H. J. C. *J. Comput. Phys.* **1997**, 23, 327
10. Darden, T. A.; York, D. M.; Pedersen, L. *J. Chem. Phys.* **1993**, 98, 10089.
11. Liu, Z.; Sun, C.; Olejniczak, E. T.; Meadows, R. P.; Betz, S. F.; Oost, T.; Herrmann, J.; Wu, J. C.; Fesik, S. W. *Nature* **2000**, 408, 1004.

12. Sun, C.; Cai, M.; Meadows, R. P.; Xu, N.; Gunasekera, A. H.; Herrmann, J.; Wu, J. C.; Fesik, S. W. *J. Biol. Chem.* **2000**, *275*, 33777.
13. Nikolovska-Coleska, Z.; Xu, L.; Hu, Z.; Tomita, Y.; Li, P.; Roller, P. P.; Wang, R.; Fang, X.; Guo, R.; Zhang, M.; Lippman, M. E.; Yang, D.; Wang, S. *J. Med. Chem.* **2004**, *47*, 2430-2440.